



3D Finite Element and Limit Equilibrium Modeling of the Initiation of Landslides

Rajib Dey¹(✉), Sina Javankhoshdel², Amir Arsalan Jameei², and Sina Moallemi²

¹ WSP, Toronto, ON, Canada
rdey@mun.ca

² Rocscience, Toronto, ON, Canada

Abstract. Large-scale failure of riverbank slopes containing sensitive clays can occur rapidly under undrained conditions. Field observations and numerical analyses indicate that forming a quasi-horizontal shear band can develop from the toe of the slopes and initiate a progressive type of failure. In this study, a semi-horizontal localization of the maximum shear strain is captured on three-dimensional slope models using RS3 finite element software. The analyses are stopped after initiating these semi-horizontal deformation patterns because no special regularization techniques are used to model strength degrading in the softening regime. Degrading the strength parameters, in general, makes the simulations pathologically mesh-dependent. In addition, developing semi-horizontal patterns results in numerical non-convergence, indicating the initiation of global instability as the safety factor becomes less than one. In this study, the formation of the semi-horizontal pattern of maximum shear strain is investigated for two different sizes of toe erosion models. In addition, slope stability analyses are carried out using 3D limit equilibrium software of Slide3D at the stages where the non-convergence takes place. The results are compared for different toe erosion models and different solution methods.

1 Introduction

Spread type landslide in sensitive clays is well-known due to their horst and graben shapes (Fig. 1). Landslides are triggered near the toe of slopes where the failure surfaces or shear zones progress up quasi-horizontally into the deposit (Demers et al., 2014). Because of the significant displacement, the soil above the failure surfaces starts moving laterally, forming several horst and graben-shaped blocks that slide (Fig. 1). The shear strains are localized around the surfaces of the horsts and grabens with minimal strains inside these blocks. The movement of the soil occurs rapidly, which indicates that the pore-fluid pressure generated during the landslide does not have sufficient time to dissipate in the undrained condition.

Researchers show that a weak horizontal layer in large-scale bank slopes results in progressive upward failure surfaces (Carson, 1977). Erosion, excavation, or small slides near the riverbank lead to initiating the horizontal shear band and developing a subsequent progressive failure mechanism (Locat et al., 2011; Quinn et al., 2011). The

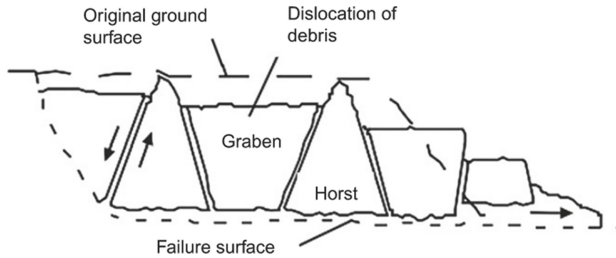


Fig. 1. Sketch of spread-type landslides in sensitive clays (after Locat et al. 2011)

progressive failure is associated with strain softening, where the strength parameters degrade during the course of deformation (Bernander, 2000). Locat et al. (2011) and Quinn et al. (2011) showed that failure generally initiates near the toe of the slope in the form of shear bands and propagates horizontally into the intact deposit. Global instability of the slope occurs when the length of the shear bands becomes sufficiently large such that the downward unbalanced force causes shear failure in the soil mass. As a result, extensive strains and displacements are developed around the quasi-horizontal shear band zones, and the soil above displaces almost laterally, forming horsts and grabens. This formation results from the progressive failure of an extensive part of the soil mass above the developed failure surface (Dey et al., 2015).

Most studies dealing with large-scale slope landslides in the form of quasi-horizontal failure surfaces focus on 2D simulations. It should be noted that accurate modeling of landslides should consider finite deformations. Dey et al. (2015) studied the problem of large-scale landslides using the Coupled Eulerian-Lagrangian (CEL) approach incorporated in Abaqus FE software for large deformations. An attempt was recently made to model and compare the initiation of propagation of quasi-horizontal failure surfaces using RS2 and RS3 software (Rocscience, 2021) in 2D plain strain and 3D configurations (Dey and Javankhoshdel, 2021a, b).

There need to be more studies in the literature that investigate the behaviour of large-scale landslides in full 3D models. Therefore, this study aimed to capture the failure initiation using the 3D Finite Element (FE) software RS3 (Rocscience, 2023). Dey and Javankhoshdel (2021) compared the safety factors of large-scale landslides using FE and LE analyses for different stages of the problem. However, the 3D factor of safety has yet to be investigated. For 3D modeling, two different models are investigated in this study. The first model was an extrusion of a 2D model where erosion was modeled throughout the entire length of the toe by reducing the strength. The second model was an extrusion of a 2D model with the erosion of a 10 m by 10 m area at the center of the toe. The second model represents a more realistic scenario because toe erosion occurs at a limited area rather than the entire toe length. For both cases, the safety factors of 3D LE and 3D FE analyses are compared for the first stage, where there is no erosion, to validate the results of the 3D LE analysis. Then, for the stage of the landslide initiation, in both 3D model scenarios, LE analyses are carried out to compare the safety factors of models with different erosion sizes.

1.1 Problem Definition

In this study, an extruded configuration of a 2D model shown in Fig. 2 (After Dey et al. 2015) is used to create the 3D models. The slope of the riverbank is $\beta = 30^\circ$, and the thickness of the crust below the ground surface is $H_c = 3\text{ m}$. A thick layer of sensitive clay with a thickness of $H_{st} = 16\text{ m}$ is located under the crust layer, followed by a thick base layer of stiff clay. Only 3m of this thick layer is modelled because depths beyond 3m do not have a significant effect on the results. For the sake of simplicity, the groundwater table is assumed to be located at the ground surface, and the river is full. It is assumed that the progressive failure is initiated by erosion of the toe of the riverbank slope. In the FE analyses, the erosion is modelled by weakening a block of soil near the toe of the slope, as shown by a shaded area in Fig. 2 (eroded block).

Figure 3a shows a complete extruded configuration of Fig. 2. The red region in Fig. 3a is the toe block that is progressively eroded. In Fig. 3a, b limited zone of erosion is assumed. The out-of-plane length in both models is 100m, and the red region in Fig. 3b is 10 m x 10 m.

Laboratory tests show that the undrained shear strength of sensitive clays decreases with the accumulation of plastic shear strains (e.g., Bernander, 2000). Following Anastopoulos et al. (2007), it is assumed that a non-localized pattern of shear strains develops throughout the whole depth of the soil specimen until it reaches the peak strength. After that, a softening behaviour is expected where the shear strength decreases with shear strain in a localized pattern. For the sake of simplicity, it is assumed in this study that the sensitive clay follows an elastic-brittle plastic behaviour as shown in Fig. 4. According to Fig. 4, the peak shear stress drops to a mobilized (residual) shear stress when the strain becomes more significant than the shear strain at the peak. The authors are aware of the effect of the shape of strain-softening curves (Dey et al., 2016); however, it is beyond the scope of this study.

Layers of the soil obey either an elastic-perfectly plastic or an elastic-brittle plastic behaviour using the Tresca yield function. Table 1 shows the material parameters. It is worth mentioning that numerical simulations of materials with brittle behaviour are commonly too sensitive to mesh sizes in the post-localized region. Different regularization techniques are used in the literature to remedy the issue, which is out of the scope of this study. This study focuses only on the initiation of the failure and not on a continuing progressive failure. The material constants were kept from a series of laboratory tests, interpretation of test data, and numerical studies on landslides in sensitive clays available in the literature (Dey et al. 2015, 2016).

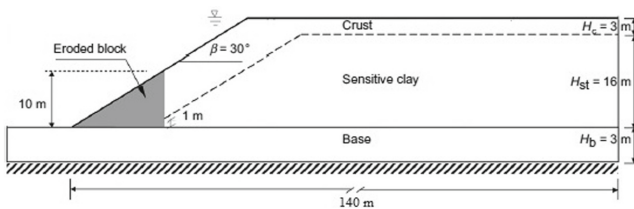


Fig. 2. The base model considered in this study (After Dey et al., 2015)

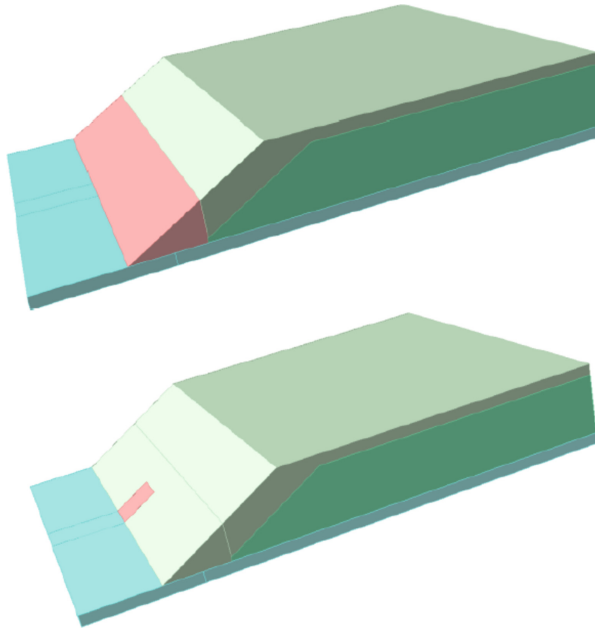


Fig. 3. The extruded version of Fig. 2 with a) a complete eroded region of the toe, b) a 10 m x 10 m eroded section of the toe

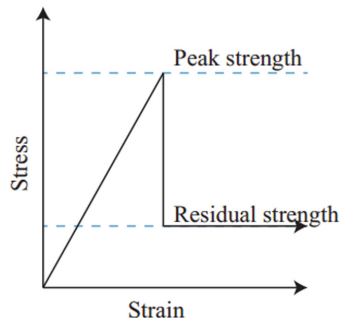


Fig. 4. Elastic-brittle plastic material model

2 Analyses and Results

Analyses are conducted in different stages. In the first stage, the material properties of the eroded block were assumed to be the same as the crust material with an elastic-ideal plastic behaviour. In other words, no erosion is considered in the first stage. In the subsequent stages, erosion is addressed by reducing the weight, strength parameters, and Young Modulus. The reduction is applied at the beginning of the subsequent stages. It is also assumed that the erosion occurred relatively fast, such that deformations are in an undrained condition. It should be noted that non-convergence criterion is used to report

Table 1. Material parameters

Parameters	Values		
	Sensitive Clay	Crust	Base
Peak undrained shear strength, S_u , kPa	37.5	60	-
Residual undrained shear strength, S_{ur} , kPa	7.5	60	-
Young's Modulus, E , MPa	7.5	10	100
Poisson ratio, ν	0.495	0.495	0.495
Unit Weight, γ , kPa	18	19	21

the failure. The solution's non-convergence is considered a condition of failure in some studies (e.g., Griffiths & Lane, 1999).

In the FE analyses, the strength and stiffness of the eroded blocks were gradually reduced, as mentioned earlier. In the study presented by Dey and Javankhoshdel (2021), the eroded block was assumed to be elastic, and erosion was modeled by reducing the unit weight and Young's modulus. However, the elastic assumption for the eroded blocks seems unrealistic. Therefore, in this study, the undrained shear strength is also reduced in addition to the unit weight and young modulus. It is worth mentioning that the reduction is applied at the beginning of each stage and not progressively throughout the simulations.

2.1 3D FE Analysis

2.1.1 Full Extruded Model with a Complete Eroded Block

As is shown in Fig. 3a and explained earlier, a complete extruded configuration of the 2D model of Fig. 2 is used for the 3D FE simulations. Figure 5b shows a qualitative pattern of the total displacement for the stage where non-convergence is captured. This stage is associated with a 5% reduction in strength and stiffness. As mentioned earlier, non-convergence has been chosen as an indicator of failure initiation in this study. Figure 5b illustrates how the maximum displacement extends from the eroded block to the crest and in the slope.

Figure 6 shows the maximum shear strain distribution when non-convergence is captured. This figure shows the development of the localized shear strain from the eroded

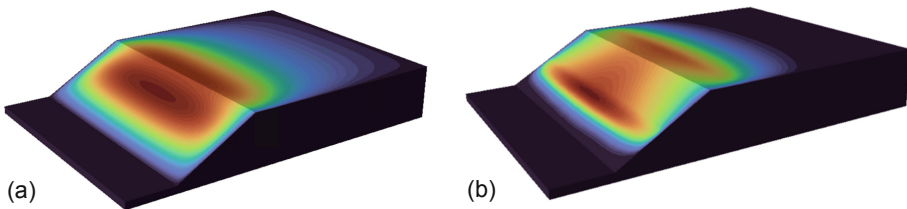


Fig. 5. Schematic pattern of the total displacement of the model with an entirely eroded toe at a) 0% and b) 5% reduction of strength and stiffness

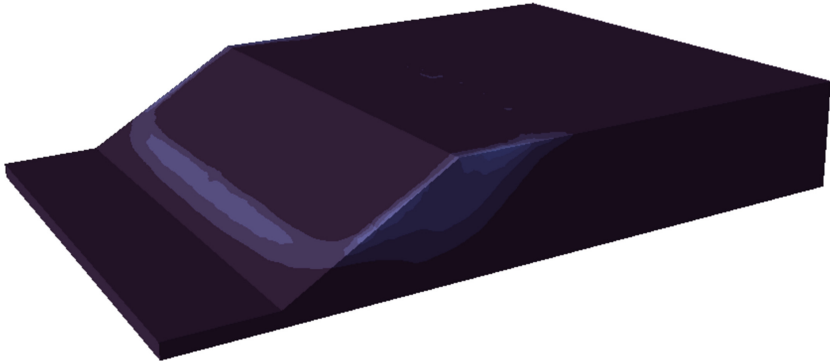


Fig. 6. Schematic pattern of the maximum shear strain of the model with an entirely eroded toe at a 5% reduction of strength and stiffness

block towards the crest of the model. The localized pattern of shear strain reaches the sides of the model because the sides are restrained against movements.

2.1.2 The Model with a 10 m x 10 m Eroded Block

This model consists of a 10 m x 10 m block of eroded materials. Figure 7 shows a qualitative pattern of the total displacement when non-convergence is captured and how the maximum displacement extends from the eroded block to the sides of the block and into the crest. Compared to Fig. 5b, the maximum displacements are concentrated towards the middle of the slope because of the presence of a limited zone rather than a larger zone of the eroded materials.

Both models, i.e., the model that contains a 10 m x 10 m eroded block (Fig. 3b) and the model with a complete extruded eroded block, show that the non-convergence (initiation of the failure) occurs at a 5% reduction of strength and stiffness. Figure 8 displays the maximum shear strain distribution of the model with a 10 m x 10 m eroded block at a 5% reduction of strength and stiffness. This figure depicts the development of the eroded block's maximum shear strain towards the model's crest, which is more

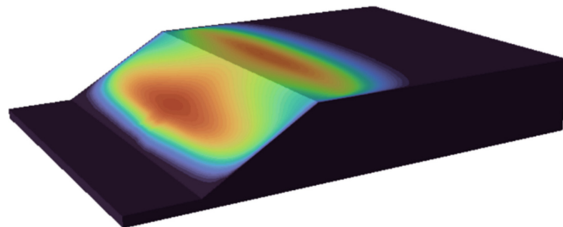


Fig. 7. Schematic pattern of the total displacement of the model with a 10 m x 10 m eroded block at a 5% reduction of strength and stiffness

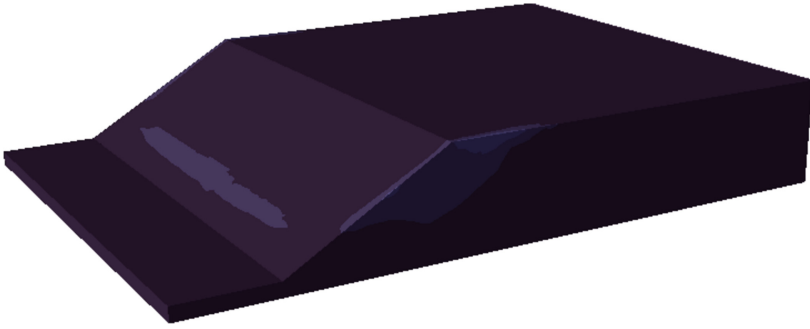


Fig. 8. Schematic pattern of the maximum shear strain of the model with a 10 m x 10 m eroded block at a 5% reduction of strength and stiffness

pronounced at the middle of the slope than the one with the model with an entirely eroded toe.

2.2 Factor of Safety Calculations

Shear Strength Reduction Method (Hammah et al. 2004) is carried out in the RS3 software to calculate the Reduction Factor (Factor of Safety, FS) for stage one of the model where there is no erosion - the obtained FS using the FE analysis of RS3 is 1.66. Figure 9 Shows the Maximum shear strain contours corresponding to this FS for different contour planes across the model.

Slide3 software (Rocscience, 2023) is also used for the same model and stage to calculate FS using the Limit Equilibrium Method (LEM). The general limit equilibrium method, together with the spline surface shape and Particle Swarm Optimization (PSO)

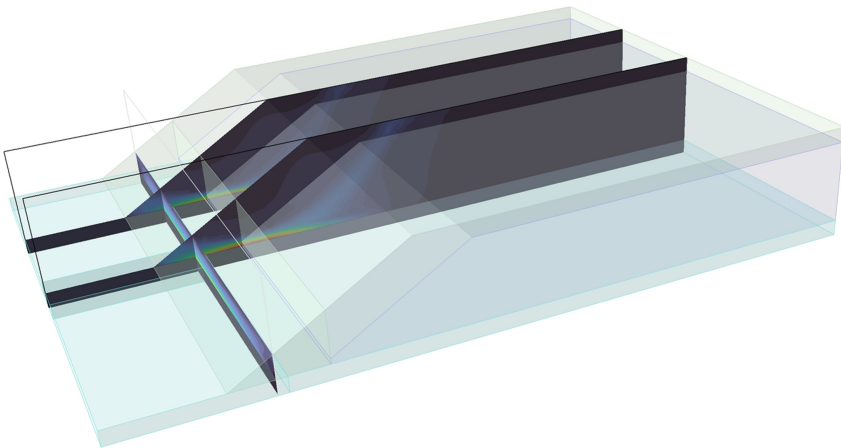


Fig. 9. Maximum shear strain contour planes for FS = 1.66

FS: 1.713

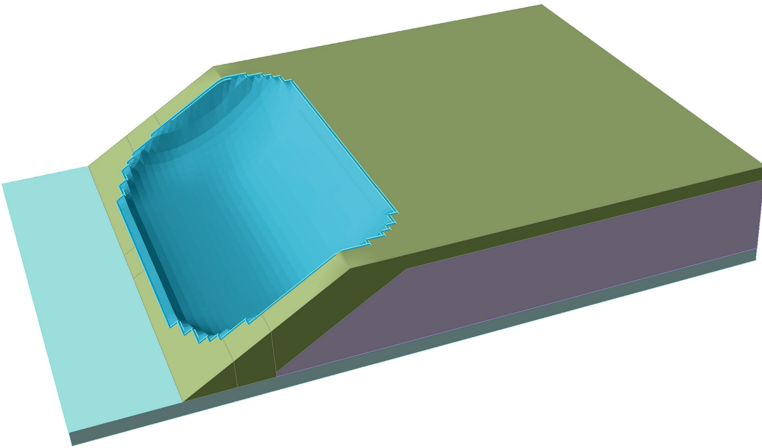


Fig. 10. The critical slip surface and FS for the 3D LE analysis

plus surface optimization techniques, are used to calculate FS in the Slide3 software. FS calculated using Slide3 is 1.71, which agrees with the 3D FE result. The result of the 3D LE model is shown in Fig. 10.

As shown in Sect. 3.1, the entirely eroded model and the model with a 10 m x 10 m eroded block reached non-convergence at a 5% reduction of strength and stiffness. A 3D LE analysis was carried out at this stage to assess the difference in FS values between these two models. Figures 11a and b show the FS of the model with an entirely eroded block and the model with a 10 m x 10 m eroded block, respectively, at a 5% reduction of strength and stiffness. Both models reached the failure ($FS < 1$) with $FS = 0.80$ for the model with a limited zone of erosion versus $FS = 0.72$ for the model with the entirely eroded block, which shows the influence of the size of the eroded block on the FS value. Figures 11a and b also depict the critical slip surface.

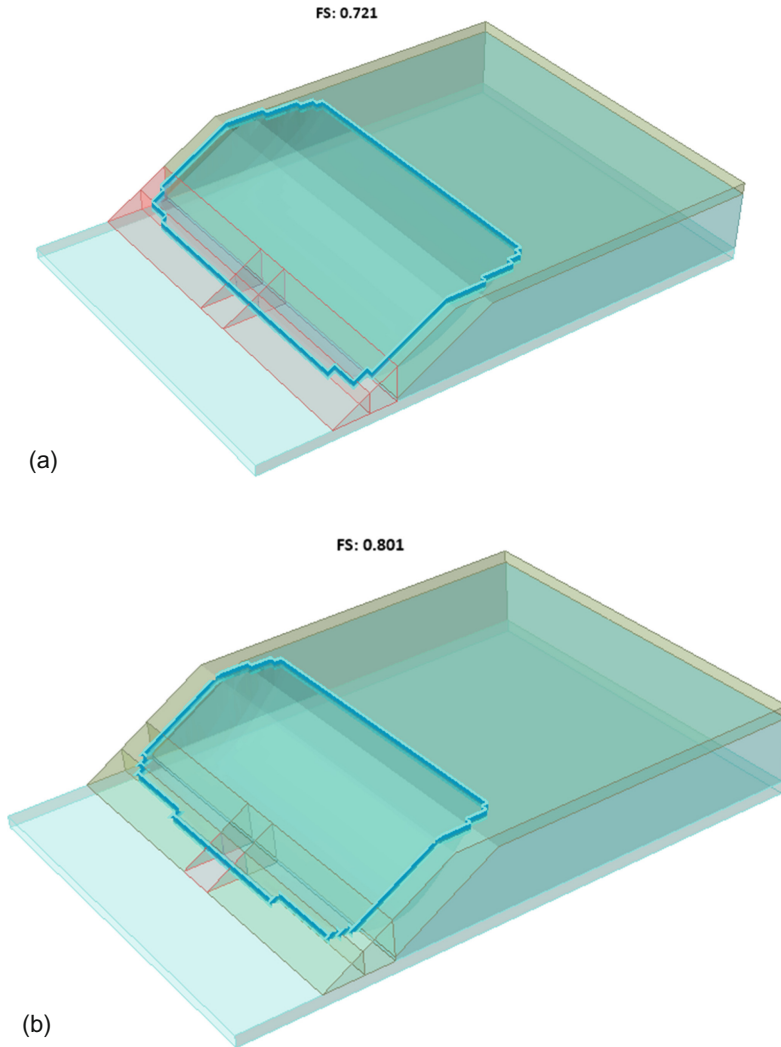


Fig. 11. The critical slip surface and its corresponding FS for a) the entirely eroded model, and b) the model with a 10 m x 10 m eroded block

3 Conclusion

The results obtained from this study indicate that 3D FE models considering strain softening could capture the propagation of failure surfaces due to erosion. The safety factor obtained from the FE model is smaller than the one of the LE analysis. Modeling of toe erosion also influences overall FS and failure surface propagation. Although the outcome of this 3D FE study is promising for modeling the initiation of spread-type landslides, significant work will be required in order to overcome the limitations of the present study.

References

- Anastasopoulos, I., Gazetas, G., Bransby, M. F., Davies, M. C. R. & El Nahas, A. 2007. Fault rupture propagation through sand: finite-element analysis and validation through centrifuge experiments. *J. Geotech. Geoenviron. Engng*, ASCE 133, No. 8, 943–958.
- Bernander, S. 2000. Progressive failure in long natural slopes: formation, potential extension and configuration of finished slides in strain-softening soils. Licentiate thesis, Luleå University of Technology, Luleå, Sweden.
- Carson, M. A. 1977. On the retrogression of landslides in sensitive muddy sediments. *Can. Geotech. J.* 14, No. 4, 582–602.
- Demers, D., Robitaille, D., Locat, P. & Potvin, J. 2014. Inventory of large landslides in sensitive clay in the province of Quebec, Canada: preliminary analysis. In *Landslides in sensitive clays – from geosciences to risk management* (eds J.-S. L’Heureux, A. Locat, S. Leroueil, D. Demers and J. Locat), pp. 77–89. Dordrecht, the Netherlands: Springer.
- Dey, R., and Javankhoshdel, S. 2021a. 2D and 3D FEM modeling of the initiation of progressive landslides. In *The Evolution of Geotech-25 Years of Innovation* (pp. 330–336). CRC Press.
- Dey, R., and Javankhoshdel, S. 2021b. 3D FEM modeling of the initiation of progressive landslides. Canadian Geotechnical Conference, GeoNiagara, Niagara Falls, On, Canada.
- Dey, R., Hawlader, B., Phillips, R. and Soga, K., 2015. Large deformation finite-element modelling of progressive failure leading to spread in sensitive clay slopes. *Géotechnique*, 65(8), pp.657–668.
- Dey, R., Hawlader, B., Phillips, R. and Soga, K., 2016. Modeling of large deformation behaviour of marine sensitive clays and its application to submarine slope stability analysis. *Canadian Geotechnical Journal*, 53 (7).
- Griffiths, D. V. & Lane, P. A. (1999). Slope stability analysis by finite elements. *Géotechnique* 49, No. 3, 387–403.
- Hammah, R.E., Curran, J.H., Yacoub, T.E., and Corkum, B., 2004, Stability Analysis of Rock Slopes using the Finite Element Method. In *Proceedings of the ISRM Regional Symposium EUROCK 2004 and the 53rd Geomechanics Colloquy*, Salzburg, Austria.
- Locat, A., Leroueil, S., Bernander, S., Demers, D., Jostad, H.P. & Ouehb, L. 2011. Progressive failures in eastern Canadian and Scandinavian sensitive clays. *Can. Geotech. J.* 48, No. 11, 1696–1712.
- Quinn, P. E., Diederichs, M. S., Rowe, R. K. & Hutchinson, D. J. 2011. A new model for large land-slides in sensitive clay using a fracture mechanics approach. *Can. Geotech. J.*, 48, No. 8, 1151–1162.
- Rocscience Inc. 2021. RS3 – 3D Finite Element Analysis. www.rocscience.com, Toronto, Ontario, Canada.
- Rocscience Inc. 2023a. RS3 – 3D Finite Element Analysis. www.rocscience.com, Toronto, Ontario, Canada.
- Rocscience Inc. 2023b. Slide3D – 3D Limit Equilibrium Analysis. www.rocscience.com, Toronto, Ontario, Canada.

Open Access This chapter is licensed under the terms of the Creative Commons Attribution-NonCommercial 4.0 International License (<http://creativecommons.org/licenses/by-nc/4.0/>), which permits any noncommercial use, sharing, adaptation, distribution and reproduction in any medium or format, as long as you give appropriate credit to the original author(s) and the source, provide a link to the Creative Commons license and indicate if changes were made.

The images or other third party material in this chapter are included in the chapter's Creative Commons license, unless indicated otherwise in a credit line to the material. If material is not included in the chapter's Creative Commons license and your intended use is not permitted by statutory regulation or exceeds the permitted use, you will need to obtain permission directly from the copyright holder.

